JACS
JOURNAL OF THE AMERICAN CHEMICAL SOCIETY
Article
pubs.acs.org/JACS

Robust, Chiral, and Porous BINAP-Based Metal–Organic Frameworks for Highly Enantioselective Cyclization Reactions

Takahiro Sawano, Nathan C. Thacker, Zekai Lin, Alexandra R. McIsaac, and Wenbin Lin*

Department of Chemistry, University of Chicago, 929 E. 57th Street, Chicago, Illinois 60637, United States

Supporting Information

ABSTRACT: We report here the design of BINAP-based metal–organic frameworks and their postsynthetic metalation with Rh complexes to afford highly active and enantioselective single-site solid catalysts for the asymmetric cyclization reactions of 1,6-enynes. Robust, chiral, and porous Zr-MOFs of UiO topology, BINAP-MOF (**I**) or BINAP-dMOF (**II**), were prepared using purely BINAP-derived dicarboxylate linkers or by mixing BINAP-derived linkers with unfunctionalized dicarboxylate linkers, respectively. Upon metalation with $Rh(nbd)_2BF_4$ and $[Rh(nbd)Cl]_2/AgSbF_6$, the MOF precatalysts **I**·$Rh(BF_4)$ and **I**·$Rh(SbF_6)$ efficiently catalyzed highly enantioselective (up to 99% ee) reductive cyclization and Alder-ene cycloisomerization of 1,6-enynes, respectively. **I**·Rh catalysts afforded cyclization products at comparable enantiomeric excesses (ee's) and 4–7 times higher catalytic activity than the homogeneous controls, likely a result of catalytic site isolation in the MOF which prevents bimolecular catalyst deactivation pathways. However, **I**·Rh is inactive in the more sterically encumbered Pauson–Khand reactions between 1,6-enynes and carbon monoxide. In contrast, with a more open structure, Rh-functionalized BINAP-dMOF, **II**·Rh, effectively catalyzed Pauson–Khand cyclization reactions between 1,6-enynes and carbon monoxide at 10 times higher activity than the homogeneous control. **II**·Rh was readily recovered and used three times in Pauson–Khand cyclization reactions without deterioration of yields or ee's. Our work has expanded the scope of MOF-catalyzed asymmetric reactions and showed that the mixed linker strategy can effectively enlarge the open space around the catalytic active site to accommodate highly sterically demanding polycyclic metallocycle transition states/intermediates in asymmetric intramolecular cyclization reactions.

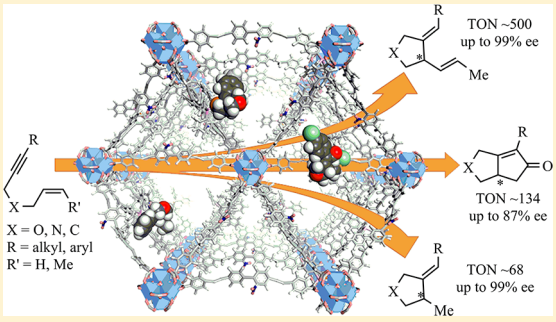

INTRODUCTION

Metal–organic frameworks (MOFs) are an interesting class of hybrid porous crystalline materials with potential applications in many areas such as gas storage,[1] chemical sensing,[2] biomedical imaging,[2a,3] drug delivery,[4] nonlinear optics,[5] and catalysis.[6,7] MOFs are particularly advantageous over other materials in their versatility as many features, including their functional groups, pore sizes, shapes, and dimensionalities, may be readily fine-tuned.[6a] In particular, highly efficient and recyclable heterogeneous catalysts have been synthesized by incorporating catalytic sites into the organic bridging ligands.[7b,c,k] In the past few years, the UiO family of MOFs with the $Zr_6(\mu_3\text{-}O)_4(\mu_3\text{-}OH)_4$ secondary building units (SBUs) and linear dicarboxylate organic linkers has particularly provided an ideal platform for designing highly efficient MOF catalysts because of their stability in a broad range of solvents and under harsh reaction conditions.[8] In this context, we recently reported a robust and porous BINAP-MOF of UiO topology and its postsynthetic metalation with Rh- and Ru-complexes to catalyze a range of asymmetric reactions including the 1,4-addition of aryl boronic acids, 1,2-addition of $AlMe_3$, and hydrogenation of ketones and alkenes.[7e,9] Although several examples of asymmetric reactions with chiral MOFs have been reported,[7f,h,j,10] the applications of MOFs in effecting useful asymmetric organic transformations remain a great challenge, in part due to the requirement of large open channels and pores while maintaining the chiral environment around the catalytically active site.

Transition-metal-catalyzed cyclization reactions provide an efficient route to complex polycyclic products from simple, readily available acyclic compounds under mild conditions.[11] In particular, asymmetric cyclization reactions of 1,6-enynes provide a powerful method to construct chiral carbon–carbon bonds in a stereoselective and atom economical fashion.[12] Chiral, five-membered rings resulted from cyclization reactions are important structural components found in a number of natural products and biologically active compounds.[13] Rh-BINAP complexes were found to efficiently catalyze asymmetric intramolecular reactions of 1,6-enynes: Krische and co-workers reported highly effective reductive cyclizations,[14] whereas Zhang and co-workers demonstrated highly enantioselective Alder-ene cycloisomerization.[15] Rh-BINAP catalysts were also shown by Jeong and co-workers to catalyze asymmetric Pauson–Khand reactions between 1,6-enynes and carbon monoxide.[16,17]

Received: February 7, 2015
Published: September 3, 2015

ACS Publications © 2015 American Chemical Society

DOI: 10.1021/jacs.5b09225
J. Am. Chem. Soc. 2015, 137, 12241–12248

As transition-metal-catalyzed cyclization reactions typically go through rigid polycyclic metallocycle transition states/intermediates, they require significantly more space around the metal centers for the catalytic reactions to proceed. Consequently, MOF catalysts have not been applied to stereoselective cyclization reactions.[18] Herein we report the first example of MOF-catalyzed enantioselective cyclization reactions using BINAP-MOF (**I**) and BINAP-doped MOF (BINAP-dMOF, **II**) catalysts (Figure 1). We find that Rh-functionalized BINAP-MOF (**I**·Rh) readily catalyzed highly enantioselective reductive cyclization and Alder-ene cycloisomerization of 1,6-enynes, but did not catalyze the Pauson–Khand cyclization between 1,6-enynes and CO. In contrast, BINAP-dMOF·Rh (**II**·Rh) readily catalyzes Pauson–Khand cyclization reactions between 1,6-enynes and CO with significantly enhanced activity over the homogeneous catalyst. Doping BINAP-derived linkers into the UiO MOF built from a less sterically demanding dicarboxylate linker thus presents a novel strategy for increasing catalytic activities of MOFs: the resultant large open channels not only facilitate substrate/product diffusion but also provide reaction space to accommodate sterically demanding transition states.

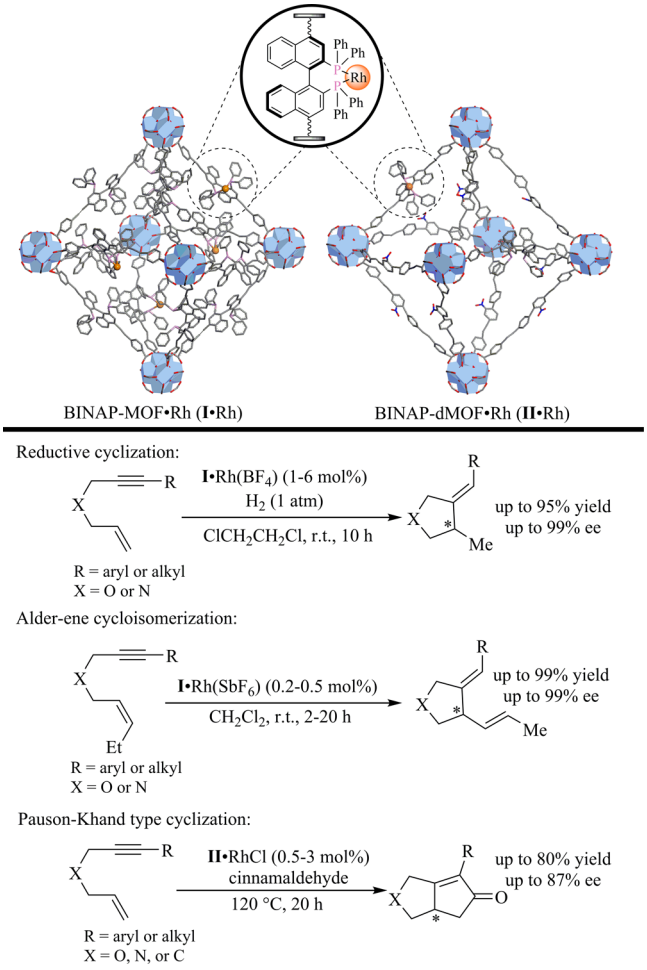

Figure 1. MOF materials as single-site solid catalysts for a broad range of asymmetric cyclization reactions.

RESULTS AND DISCUSSION

BINAP-MOF (**I**) of the framework formula $Zr_6(OH)_4O_4(\mathbf{L1})_6$ was synthesized via our previously published procedure by a solvothermal reaction between 4,4′-bis(4-carboxyphenylethynyl)BINAP ($H_2\mathbf{L1}$), $ZrCl_4$, and trifluoroacetic acid (TFA) in dimethylformamide (DMF).[7e] Post-synthetic metalation of **I** was achieved by addition of 1 equiv $Rh(nbd)_2BF_4$ or 0.5 equiv $[Rh(nbd)Cl]_2$ to **I** (relative to BINAP moieties in **I**). Inductively coupled plasma mass spectrometry (ICP-MS) analyses of the Zr:Rh ratios of the digested MOFs afforded Rh loadings of 33% for **I**·$Rh(BF_4)$ and 18% for **I**·RhCl. Analysis of powder X-ray diffraction (PXRD) patterns found **I** maintained its crystallinity after metalation with Rh (Figure 2a).

Due to the positional disorder and incomplete metalation of the BINAP moiety, investigation of the Rh-coordination environment could not be performed by traditional crystallographic techniques. X-ray absorption fine structure (XAFS) spectroscopy at the Rh K-edge was used to investigate the local

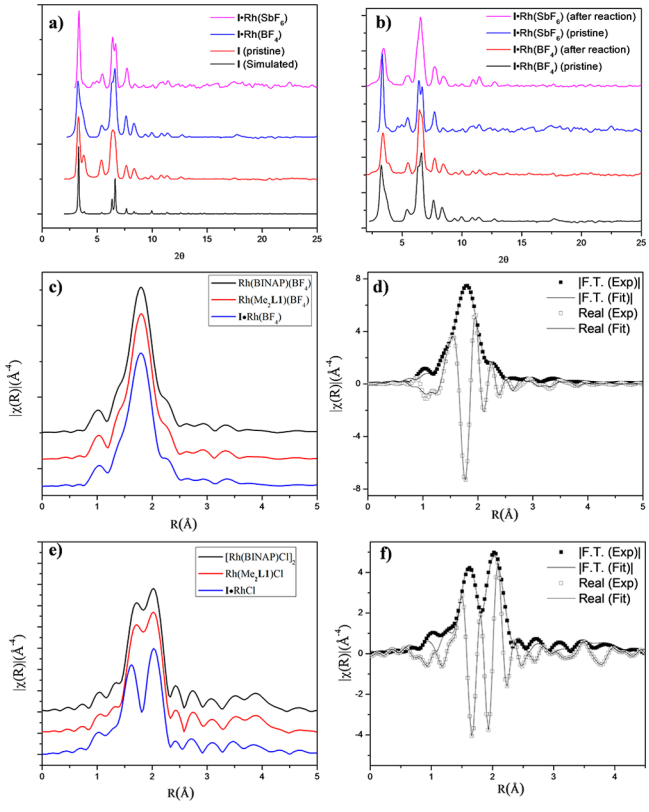

Figure 2. (a) PXRD patterns of **I** (simulated from the CIF file, black; freshly prepared **I**, red), **I**·$Rh(BF_4)$ (blue), and **I**·$Rh(SbF_6)$ (pink). (b) PXRD patterns of freshly prepared **I**·$Rh(BF_4)$ (black), **I**·$Rh(BF_4)$ recovered from reductive cyclization reaction with **1a** (red), freshly prepared **I**·$Rh(SbF_6)$ (blue), and **I**·$Rh(SbF_6)$ recovered from Alder-ene reaction with **3a** (pink). (c) A comparison of EXAFS data for **I**·$Rh(BF_4)$, $Rh(Me_2\mathbf{L1})BF_4$, and Rh(BINAP) BF_4. (d) EXAFS data (squares) and best fits (lines) for **I**·$Rh(BF_4)$. Data are displayed in *R*-space containing both magnitude of Fourier transform and real components. An *R*-factor of 0.01 was obtained for the fit. (e) A comparison of EXAFS data for **I**·RhCl, $Rh(Me_2\mathbf{L1})Cl$, and the $[Rh(BINAP)Cl]_2$ dimer. (f) EXAFS data (squares) and best fits (lines) for **I**·RhCl. Data are displayed in *R*-space containing both magnitude of Fourier transform and real components. An *R*-factor of 0.02 was obtained for the fit.

DOI: 10.1021/jacs.5b09225
J. Am. Chem. Soc. 2015, 137, 12241–12248

coordination environment of Rh in **I**·Rh(BF_4), **I**·RhCl, Rh(Me_2**L1**)BF_4, Rh(Me_2**L1**)Cl, Rh(BINAP)BF_4, and [Rh(BINAP)Cl]$_2$. **I**·Rh(BF_4) and Rh(Me_2**L1**)BF_4 were fitted with the crystal structure of Rh(BINAP)BF_4 (Figures 2d and S9–11). **I**·RhCl was fitted with a monomeric model where the Rh coordination sphere is occupied by BINAP, chloride, and a THF molecule (Figures 2f and S14). The spectra for Rh(Me_2**L1**)Cl was fitted with the crystal structure of dimeric [Rh(BINAP)Cl]$_2$ (Figures S12 and S13). The details of fitting procedures and results are provided in the SI.

We first explored asymmetric intramolecular cyclization of enynes using **I**·Rh(BF_4). Krische and co-workers reported Rh-catalyzed reductive cyclization using hydrogen as a terminal reductant.[14] At 1 mol % **I**·Rh(BF_4) loading (based on Rh), 1,6-enyne **1a** was converted to monoalkylidene furan **2a** in 68% yield and 94% ee in a H_2 atmosphere at rt (Table 1, entry 1).

Table 1. Asymmetric Reductive Cyclization of 1,6-Enynes[a]

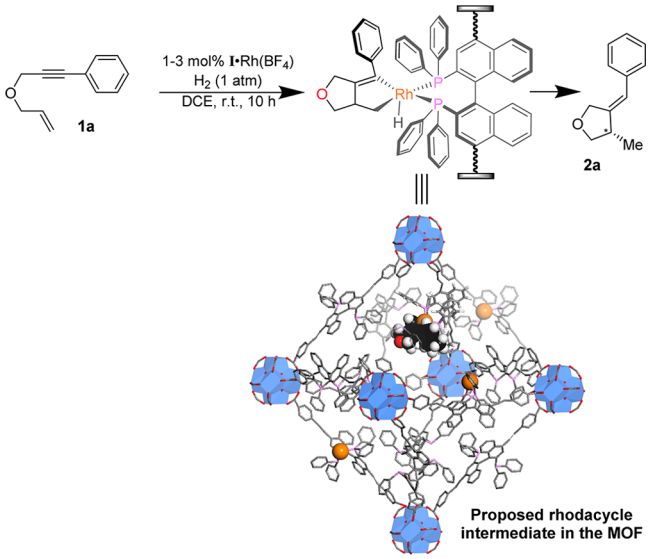

entry	catalyst	Rh-loading (mol %)	yield (%)[b]	ee (%)[c]
1	**I**·Rh(BF_4)	1	68	94
2[d]	Rh(Me_2**L1**)BF_4	1	10	91
3	**I**·Rh(BF_4)	3	95 (90)[e]	95

[a]Reaction conditions: **1** (1 equiv), catalyst, H_2 (1 atm) at rt for 10 h. [b]Determined by ^{1}H NMR integration with CH_3NO_2 as an internal standard. [c]Determined by chiral HPLC. [d]Catalyst was generated *in situ*. [e]Isolated yield.

This cyclization reaction likely proceeded through the rhodacycle as proposed by Krische and co-workers (Table 1). Under similar conditions, the homogeneous control Rh(Me_2**L1**)BF_4 was significantly less active affording the cyclized product in only 10% yield and 91% ee (Table 1, entry 2). The enhanced catalytic activity of **I**·Rh(BF_4) over Rh(Me_2**L1**)BF_4 (by ~7 times) is likely due to the prevention of multimolecular catalyst deactivation via catalytic site isolation. At 3 mol % loading of **I**·Rh(BF_4), **2a** was obtained in nearly quantitative yield and 95% ee (Table 1, entry 3).

Next, we examined the substrate scope of 1,6-enynes in the **I**·Rh(BF_4)-catalyzed reductive cyclization reactions (Table 2). Three mol % of **I**·Rh(BF_4)-catalyzed cyclization of the unsubstituted 1,6-enyne **1b** afforded monoalkylidene furan **2b** in 89% yield and 96% ee (Table 2, entry 2). 1,6-enynes bearing either electron-donating groups or bulky substituents formed

Table 2. Scope of Asymmetric Reductive Cyclization Reaction with I·Rh(BF_4)[a]

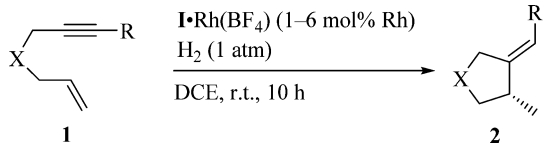

entry	X	R	Rh-loading (mol %)	yield (%)[b]	ee (%)[c]
1	O	4-MeC_6H_4 (**1a**)	3	95	95
2	O	C_6H_5 (**1b**)	3	89	96
3	O	4-$MeOC_6H_4$ (**1c**)	3	87	95
4	O	4-^{t}BuC_6H_4 (**1d**)	3	82	99
5	O	4-$CF_3C_6H_4$ (**1e**)	3	70	94
6	O	3,5-$Ph_2C_6H_3$ (**1f**)	1	16	88
7	NTs	CH_3 (**1g**)	3	83	67
8	NTs	C_6H_5 (**1h**)	6	99	88

[a]Reaction conditions: **1** (1 equiv), catalyst, H_2 (1 atm) at rt for 10 h. [b]Determined by ^{1}H NMR integration with CH_3NO_2 as an internal standard. [c]Determined by chiral HPLC. [d]Catalyst was generated *in situ*. Ts = *p*-toluenesulfonyl

cyclic products in high ee's and good yields (Table 2, entries 3–4). The highest ee of 99% was observed for the cyclized product **2d** that bears the bulky ^{t}Bu group. Electron-withdrawing groups have a slightly deleterious effect on yields due to formation of undesired byproducts; fortunately, the ee remains high for the cyclized product (Table 2, entry 5). For sterically cumbersome substrate **1f**, the reaction affords 16% yield, likely attributable to the slow diffusion of **1f** through the MOF and/or the limited open space in the MOF (Table 2, entry 6 vs Table 1, entry 1).[19] Substrates bearing a nitrogen tether (**1g** and **1h**) were tolerated, giving cyclized products in 83% and 99% yield, respectively (Table 2, entries 7 and 8).

The Rh-catalyzed asymmetric Alder-ene cyclization is a powerful method for generating chiral heterocycles possessing the 1,4-diene products from 1,6-enynes. The cyclized product is believed to form via the *β*-hydride elimination and reductive elimination sequence. While **I**·Rh(BF_4) efficiently catalyzed the reductive cyclization of 1,6-enynes, it was ineffective in the Alder-ene cycloisomerization (Table 3, entry 1). Instead, the **I**·Rh(SbF_6) catalyst, generated *in situ* by treating **I**·RhCl with $AgSbF_6$, afforded the cyclized 1,4-diene product in 99% yield and 99% ee (Table 3, entry 2). The less coordinating SbF_6^- anion is essential for the Alder-ene cyclization activity (Table 3, entry 3). Enhanced activity from site isolation in **I**·Rh(SbF_6) is again demonstrated when comparing the catalytic activity of **I**·Rh(SbF_6) and Rh(Me_2**L1**) (SbF_6) (Table 3, entries 2 vs 4); **I**·Rh(SbF_6) is at least 4 times more active than the homogeneous control. We believe that the Rh catalyst is significantly stabilized due to site isolation. The homogeneous catalyst is deactivated within 2 h, and prolonging the reaction time did not lead to increased product formation (Table 3, entries 4 and 5).

I·Rh(SbF_6)-catalyzed Alder-ene cycloisomerization also has excellent regioselectivity, which is surprising considering the high reactivity of both the starting enyne **3a** and the product **4a** under catalytic conditions. Zhang and co-workers reported that 1,6-enyne **3a** readily isomerized to the 1,5-enyne **3a**′ in the presence of high loading of homogeneous catalysts (>20 mol %, Scheme 1).[15a] Additionally, cycloisomerized product **4a** is susceptible to isomerization under prolonged reaction con-

DOI: 10.1021/jacs.5b09225
J. Am. Chem. Soc. 2015, 137, 12241–12248

Table 3. Asymmetric Alder-Ene Cyclization of 3a[a]

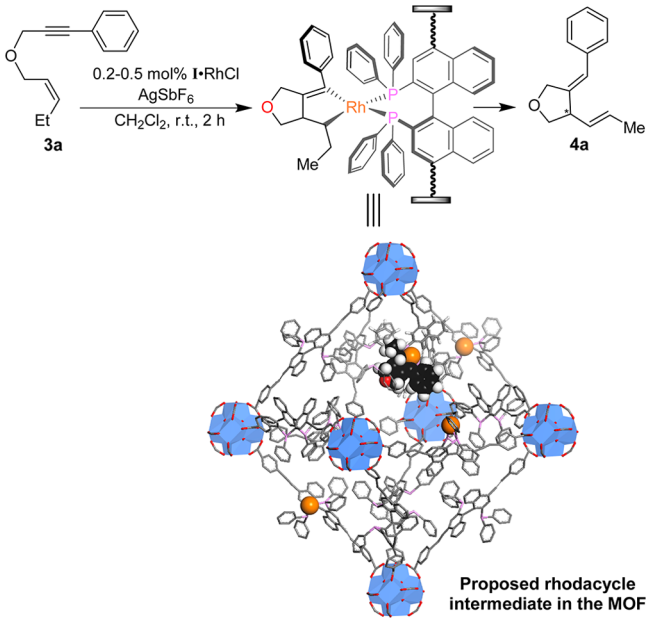

entry	precatalyst	Rh loading (mol %)	yield (%)[b]	ee (%)[c]
1[d]	I·Rh(BF_4)	0.5	0	–
2	I·Rh(SbF_6)	0.2	99 (95)[e]	99
3[d]	I·RhCl	0.2	0	–
4[f]	Rh(Me_2**L1**) (SbF_6)	0.2	26	99
5[fg]	Rh(Me_2**L1**) (SbF_6)	0.2	26	99

[a]Reaction conditions: **3a** (1 equiv), $AgSbF_6$ (10 equiv relative to Rh), catalyst at rt for 2 h. [b]Determined by ^{1}H NMR integration with CH_3NO_2 as an internal standard. [c]Determined by chiral HPLC. [d]No $AgSbF_6$ added. [e]Isolated yield. [f]Catalyst generated *in situ*. [g]Reaction time was 20 h.

Scheme 1. Commonly Observed Byproducts in the Rh-Catalyzed Alder-ene Cyclization of 1,6-Enynes

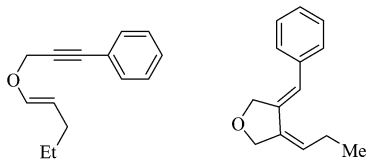

3a' (Isomerized from **3a**) **4a'** (Isomerized from **4a**)

ditions forming the more stable conjugated 1,3-diene **4a'**. Despite the enhanced catalytic activity of I·Rh(SbF_6), we did not observe isomerized byproduct **3a'** or **4a'** and only detected **3a** and **4a** in the ^{1}H NMR spectrum of the crude reaction mixture.

We subsequently explored the substrate scope for I·Rh-catalyzed Alder-ene reactions (Table 4). With 0.2 mol % catalyst, *para*-Me substituted enyne **3b** was converted to cycloisomerized product **4b** in 65% yield and 99% ee (Table 4, entry 2). Increasing the catalyst loading (0.5 mol %) and reaction time (20 h) led to quantitative yields while maintaining excellent enantioselectivity (Table 4, entry 3). At 0.5 mol % I·Rh(SbF_6) loadings, cycloisomerized products **4c** and **4d** were obtained from *para*-OMe and *para*-^{t}Bu substituted enyne **3c** and **3d** in quantitative yields and 99% ee, respectively (Table 4, entries 5 and 6). Enynes bearing electron-withdrawing groups were significantly more reactive; only 0.2 mol % catalyst loading

Table 4. Scope of Asymmetric Alder-ene Reaction with I·Rh(SbF_6)[a]

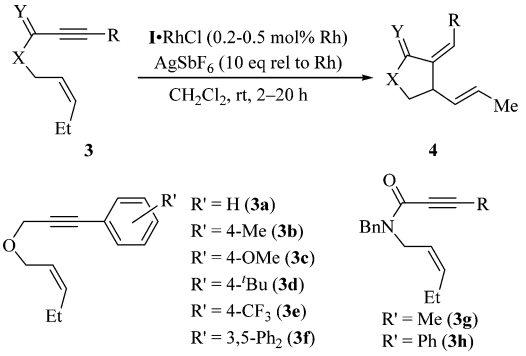

entry	3	Rh loading (mol %)	yield (%)[b]	ee (%)[c]
1	**3a**	0.2	99 (**4a**)	99
2	**3b**	0.2	65 (**4b**)	99
3[d]	**3b**	0.5	99 (**4b**)	99
4	**3c**	0.2	60 (**4c**)	99
5[d]	**3c**	0.5	99 (**4c**)	99
6[d]	**3d**	0.5	99 (**4d**)	99
7	**3e**	0.2	99 (**4e**)	99
8	**3f**	0.2	18 (**4f**)	99
9	**3g**	0.2	98 (**4g**)	99
10[d]	**3h**	0.5	99 (**4h**)	99

[a]Reaction conditions: **3** (1 equiv), $AgSbF_6$ (10 equiv relative to Rh), catalyst at rt, 20 h. [b]Determined by ^{1}H NMR integration with CH_3NO_2 as an internal standard. [c]Determined by chiral HPLC. [d]Reaction time was 20 h. Bn = Benzyl.

was needed to convert *para*-CF_3 substituted enyne **3e** to its cyclized product in quantitative yield and 99% ee in 2 h (Table 4, entry 7). For considerably larger substrate **3f**, standard reaction conditions provided only 18% yield; this is likely attributed to sluggish diffusion through the MOF and/or the insufficient open space in the MOF (Table 4, entry 8).[20] Substrates bearing a nitrogen tether (**1g** and **1h**) afford cyclized saturated N-heterocycles in excellent enantioselectivity and yields (98% and 99% yield, respectively) (Table 4, entries 9 and 10).[15d] As was observed with enyne **3a**, undesired isomerization or rearrangement was not observed from any of the I·Rh(SbF_6)-catalyzed Alder-ene reactions.

The PXRD pattern of the recovered I·Rh(BF_4) after the reductive cyclization reaction remained similar to that of freshly prepared I·Rh(BF_4); this holds true for the recovered I·Rh(SbF_6) after the Alder-ene reaction (Figure 2b). These results indicate the framework of **I** is stable under asymmetric catalytic reaction conditions. However, the recovered I·Rh(BF_4) and I·Rh(SbF_6) showed low or no catalytic activity when resubjected to reaction conditions with fresh substrates, suggesting that the BINAP-Rh complexes in the MOF slowly form stable but catalytically inactive species during the catalytic processes. Consistent with this, insignificant amounts of Rh and Zr species were leached from the MOFs as determined by ICP-MS. For the reductive cyclization with I·Rh(BF_4), 0.0% Zr and 3.7% rhodium were found in the supernatant. For the Alder-ene reaction with I·Rh(SbF_6), <0.1% of Zr and Rh species was found in the supernatant.

We turned our attention next to the even more sterically demanding asymmetric Pauson–Khand reaction with I·Rh.[16c,d] The Pauson–Khand reaction is a useful carbonylative alkene-alkyne coupling method to afford chiral bicyclic heterocycles

DOI: 10.1021/jacs.5b09225
J. Am. Chem. Soc. 2015, 137, 12241–12248

and carbocycles from relatively simple starting materials. Based on the success of using H_2 for the **I**·Rh(BF_4)-catalyzed reductive cyclization of 1,6-enynes, we were interested in effecting Pauson–Khand reactions under an atmosphere of CO with **I**·Rh. Unfortunately, our attempts at a Pauson–Khand reaction with *para*-Cl substituted enyne **1i** and CO were unsuccessful (Scheme S4).[21] The inability to perform Pauson–Khand reactions with MOF catalysts could be attributed to limited solubility and permeability of CO under the heated reaction conditions. As an alternative method to introduce CO, aldehydes may be used as both solvent and CO source for metal-catalyzed Pauson–Khand-type reactions.[16b−d] In addition to the obvious advantage of generating CO *in situ*, Shibata and co-workers found Rh-phosphine catalysts generated Pauson–Khand products in significantly higher yields using cinnamaldehyde as the CO source versus carrying out the reaction in an atmosphere of CO.[16d] Unfortunately, the **I**·Rh-catalyzed asymmetric Pauson–Khand reaction of **1i** and cinnamaldehyde **6** affords the desired bicyclic product **5i** in low yield (<5%, Figure 3a). We believe the low catalytic activity

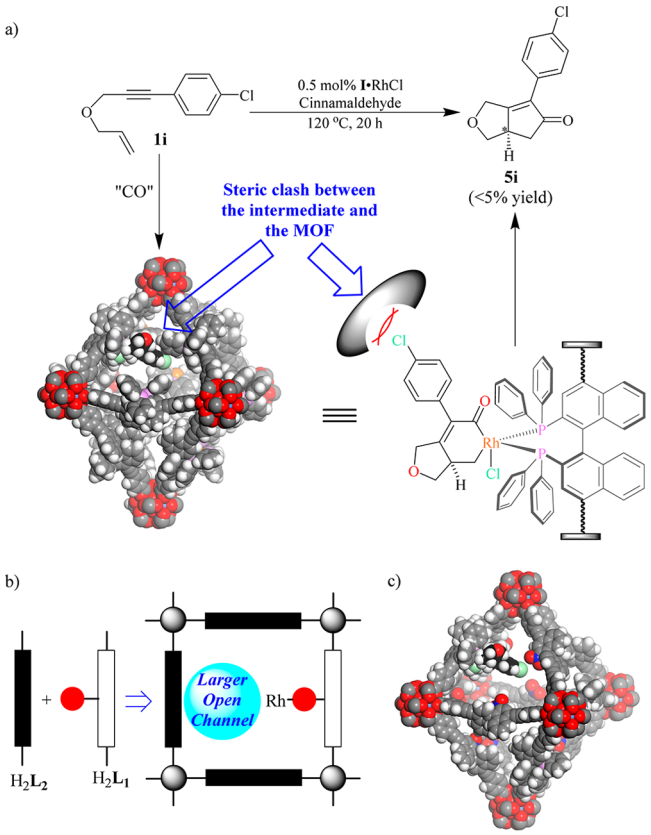

Figure 3. (a) **I**·Rh is inactive in asymmetric Pauson–Khand-type reaction of **1i** due to the steric clash between the bicyclic rhodacycle intermediate and the MOF framework. (b) Mixed-linker MOF **II** possesses larger open channels. (c) Space-filling model showing the accommodation of the bicyclic rhodacycle intermediate in larger open space in **II**·RhCl.

of **I**·Rh is resultant of insufficient reaction space required to accommodate the large bicyclic rhodacycle intermediate. To increase the reaction space through modification of the effective pore space, a new BINAP-doped MOF was prepared from a mixture of functionalized and unfunctionalized linkers of identical lengths (Figure 3b).[22]

The unfunctionalized linker H_2**L2** was prepared from 4,4′-dibromo-2-nitrobiphenyl[23] in two steps as shown in Scheme 2.

Scheme 2. Synthesis of BINAP-dMOF II Starting From 4,4′-Dibromo-2-nitrobiphenyl[a]

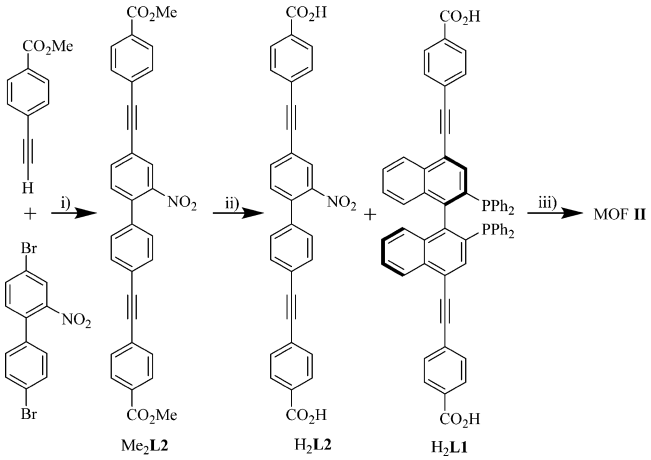

[a]Reagents: (i) $Pd(PPh_3)_4$, CuI, PPh_3, TEA, THF, 75 °C, 63% yield; (ii) NaOH, THF, EtOH, H_2O, 70 °C, 71% yield; (iii) H_2**L1**, $ZrCl_4$, TFA, DMF, 100 °C, 71% yield.

Pd-catalyzed Sonogashira reaction of 4,4′-dibromo-2-nitrobiphenyl with methyl 4-ethynylbenzoate afforded Me_2**L2** in 63% yield. Me_2**L2** was saponified under basic conditions to afford H_2**L2** in 45% overall yield. The nitro group was introduced to increase the solubility of H_2**L2**, thereby facilitating MOF crystal growth.

Due to the air-sensitive nature of H_2**L1**, solvothermal crystal growths of mixed-linker MOF (**II**) were carried out in an oxygen-free environment. A mixture of H_2**L1** (1 equiv), H_2**L2** (4 equiv), $ZrCl_4$, and TFA (75 equiv) in DMF was degassed in a glass tube, flame-sealed under vacuum, and heated at 100 °C for 7 days. MOF **II** was isolated as octahedral microcrystals in 71% yield. For comparison, the nondoped nitro-MOF, constructed from only unfunctionalized linker H_2**L2**, was synthesized under similar conditions (Scheme S2). Nitro-MOF adopts the UiO framework structure of the fcu topology by connecting the $Zr_6(\mu_3\text{-}O)_4(\mu_3\text{-}OH)_4$ SBUs with **L2** linkers. The nitro groups are disordered due to random orientations and cannot be located in the electron density map. PLATON calculations indicated the presence of 89.4% void space in the nitro-MOF. The PXRD pattern for the nitro-MOF matches that of the simulated pattern using the cif file, confirming the phase purity of the nitro-MOF (Figure 4a).

The PXRD pattern of MOF **II** is similar to that of the nitro-MOF, indicating the adoption of the UiO topology for MOF **II** (Figure 4a). Thermogravimetric analysis (TGA) showed that **II** contained 64 wt % solvent (Figure S1). The ratio of **L1** to **L2** in **II** was determined by ^{1}H NMR to be 0.13:0.87 after complete digestion of MOF **II** in K_3PO_4, D_2O, and d_6-DMSO (Figure S2). The framework formula for **II** is approximately $Zr_6(OH)_4O_4$(**L1**)$_{0.78}$(**L2**)$_{5.22}$. Attempts to determine the surface area of **II** were unsuccessful; the N_2 sorption measurements gave negligible surface areas, presumably due to framework distortion upon solvent removal.[7e,10f,24]

Postsynthetic metalation was performed by treating **II** with 1.8 equiv of $[RhCl(nbd)]_2$ (relative to **L1** equivalents in **II**, SI). The crystallinity of **II**·RhCl was maintained as evidenced by the

DOI: 10.1021/jacs.5b09225
J. Am. Chem. Soc. 2015, 137, 12241−12248

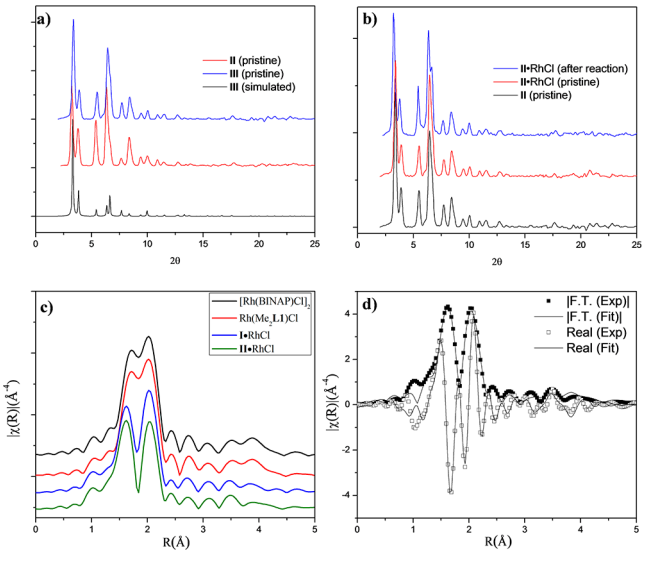

Figure 4. (a) PXRD patterns of pristine nitro-MOF (simulated from the CIF file, black; experimental, red), freshly prepared **II** (blue). (b) PXRD patterns of pristine **II** (black), freshly prepared **II**·RhCl (red), and **II**·RhCl recovered from Pauson–Khand reactions (blue). (c) A comparison of EXAFS data for **II**·RhCl, **I**·RhCl, Rh(Me$_2$**L1**)Cl, and the [Rh(BINAP)Cl]$_2$ dimer. (d) EXAFS data (squares) and best fits (lines) for **II**·RhCl. Data are displayed in *R*-space containing both magnitude of Fourier transform and real components. An *R*-factor of 0.02 was obtained for the fit.

similarity of its PXRD pattern to that of **II** (Figure 4b). ICP-MS analyses of digested **II**·RhCl samples established that 61% of **L1** has been metalated with Rh. EXAFS of **II**·RhCl was fitted with the same model of **I**·RhCl, demonstrating similar Rh local environment of **I**·RhCl and **II**·RhCl (Figures 4c and S15).

The asymmetric Pauson–Khand-type reaction of 1,6-enyne **1i** and *trans*-cinnamyl aldehyde (**6**) (60 equiv) with **II**·RhCl (0.5 mol % Rh) afforded the chiral bicyclic product **5i** in 67% yield and 80% ee (Table 5, entry 2). The inclusion of unfunctionalized **L2** linkers in **II** has created more open space around the BINAP-Rh active sites, allowing the generation of sterically demanding bicyclic rhodacycle intermediates. The

Table 5. Asymmetric Pauson–Khand-Type Reaction of 1,6-Enyne (1i)[a]

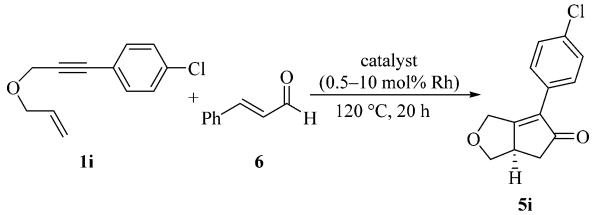

1i **6** **5i**

entry	catalyst	cat. loading (mol %)	yield (%)	ee (%)[b]
1	I·RhCl	0.5	<5[c]	–[d]
2	**II**·RhCl	0.5	67	80
3	Rh(Me$_2$**L1**)Cl	0.5	<5[c]	–[d]
4	Rh(Me$_2$**L1**)Cl	5.0	69	77
5	Rh(Me$_2$**L1**)Cl	10	84	77
6	**II**·RhCl	1.0	80	82

[a]Reaction conditions: **1i** (1 equiv), **6** (60 equiv), catalyst at 120 °C for 20 h. [b]Determined by chiral HPLC. [c]Determined by ^{1}H NMR integration. [d]Not determined

ability of **II**·RhCl in catalyzing this reaction has interesting mechanistic implications. Shibata and co-workers proposed that the cinnamaldehyde decarbonylation-Pauson–Khand reaction did not occur through the formation of CO gas as an intermediate, but instead involved a direct CO transfer between two independent Rh-mediated catalytic cycles.[16d] With the mixed-linker MOF **II**·RhCl as a single-site solid catalyst, such a direct CO-transfer mechanism cannot be operative. Our results argue in favor of the Pauson–Khand-type reaction via CO generation from cinnamaldehyde.

To further assess the impact of site isolation on the Pauson–Khand-type reaction, the activity of **II**·RhCl was compared to the homogeneous control; at 0.5 mol % catalyst loading of homogeneous Rh(Me$_2$**L1**)Cl, <5% product **5i** was obtained (Table 5, entry 3). Increasing the Rh(Me$_2$**L1**)Cl loading to 5 mol % led to the formation of **5i** in 69% yield. **II**·RhCl is thus about 10 times more active than the homogeneous control (entries 2 vs 4) and exhibits similar enantioselectivity as the homogeneous catalyst. A higher yield of **5i** (80%) was obtained when 1 mol % of **II**·RhCl was used (Table 5, entry 6).

With optimized conditions for the **II**·RhCl-catalyzed Pauson–Khand reaction of **1i** in hand, we examined the substrate scope using a series of 1,6-enynes bearing either electron-withdrawing or electron-donating substituents (Table 6). Substrates bearing electron-withdrawing substituents, such

Table 6. Asymmetric Pauson–Khand-Type Reactions of 1,6-Enynes with II·RhCl[a]

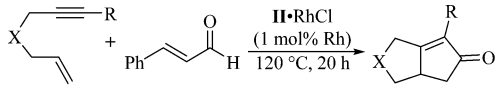

1 **6** **5**

entry	X	R	yield (%)[b]	ee (%)[c]
1	O	4-ClC$_6$H$_4$ (**1i**)	80 (**5i**)	82
2	O	4-C$_6$H$_4$CF$_3$ (**1e**)	80 (**5e**)	55
3	O	4-MeC$_6$H$_4$ (**1a**)	62 (**5a**)	67
4	O	4-OMeC$_6$H$_4$ (**1c**)	67 (**5c**)	83
5[d]	O	C$_6$H$_5$ (**1b**)	79 (**5b**)	87
6	O	4-^{t}BuC$_6$H$_4$ (**1d**)	60 (**5d**)	81
7	NTs	CH$_3$ (**1g**)	91 (**5g**)	58
8[e]	NTs	C$_6$H$_5$ (**1h**)	88 (**5h**)	10
9[e]	C(CO$_2$Me)	CH$_3$ (**1j**)	80 (**5j**)	70
10[e]	C(CO$_2$Me)	C$_6$H$_5$ (**1k**)	85 (**5k**)	12

[a]Reaction conditions: **1** (1 equiv), **6** (60 equiv), catalyst **II**·RhCl (1 mol % Rh) at 120 °C for 20 h. [b]Isolated yield. [c]Determined by chiral HPLC. [d]0.5 mol % Rh. [e]3.0 mol % Rh. Ts = *p*-toluenesulfonyl.

as *para*-Cl **1i** and *para*-CF$_3$ **1e**, afford the desired bicyclic products in good yield and modest enantioselectivity. With electron-donating substituents such as *para*-Me (**1a**) and *para*-OMe (**1c**), the Pauson–Khand products were obtained in lower yields but slightly higher ee's (Table 6, entries 3 and 4). At 0.5 mol % **II**·RhCl, unsubstituted enyne **1b** afforded the bicyclic product in 79% yield and 87% ee (Table 6, entry 5). Substrates bearing a bulky *para*-^{t}Bu substituent resulted in bicycle formation in modest yield and good ee (Table 6, entry 6). Nitrogen- and carbon-tethered substrates may also be used affording bicyclic products in good yields albeit at lower enantioselectivities (Table 6, entries 7–10).

The heterogeneous nature of **II**·RhCl was confirmed by the following experiments. PXRD of **II**·RhCl recovered from the Pauson–Khand reaction with **1i** indicated that the crystallinity

DOI: 10.1021/jacs.5b09225
J. Am. Chem. Soc. 2015, 137, 12241–12248

of **II**·RhCl was maintained throughout the course of the reaction (Figure 4b). ICP-MS analyses indicated that <0.5% Zr and 5.1% Rh species had leached into the supernatant of the **II**·RhCl-catalyzed Pauson–Khand reaction of **1i**. At 5 mol % catalyst loading, **II**·RhCl may be successfully recycled and reused for the Pauson–Khand reaction of **1i**. The yields/ee's for three consecutive runs (with recovered **II**·RhCl) are 85/78%, 83/75%, and 83/75%, respectively (Scheme S3).

CONCLUSIONS

We have developed porous and robust BINAP-based MOFs for highly active and enantioselective asymmetric cyclization reactions. The BINAP-MOF Rh catalysts are highly active in the asymmetric reductive cyclization and Alder-ene cycloisomerization, affording the cyclized products in 4–7 times higher yields than and comparably high ee's (up to 99%) to the homogeneous catalysts. However, they are inactive in more sterically demanding asymmetric Pauson–Khand-type reactions. We have introduced a mixed-linker strategy to enlarge the open space around the catalytic active sites to accommodate the sterically encumbered bicyclic rhodacycle intermediates. The BINAP-dMOF Rh catalysts, built from functionalized and unfunctionalized linkers, readily catalyzed asymmetric Pauson–Khand-type reactions at about 10 times higher activity than the homogeneous control catalyst. We also showed that the MOF catalysts are not only more active than their homogeneous counterparts but can also eliminate undesired isomerization of starting materials and products in Alder-ene cycloisomerization reactions. The MOF catalysts also provided interesting mechanistic insights into the Pauson–Khand-type reactions using cinnamaldehyde as the CO source.

Our work has for the first time demonstrated the utility of MOF catalysts in complex and sterically demanding asymmetric cyclization reactions which significantly expands the scope of MOF-catalyzed asymmetric reactions. MOFs provide a unique platform for the preparation of truly single-site solid catalysts based on molecular complexes. The site isolation of catalytically active species in MOFs prevents multimolecular catalyst deactivation, leading to higher catalytic activity over their homogeneous counterparts. By incorporating "privileged ligands"[25] into robust and porous MOFs, a new generation of single-site solid catalysts can be envisioned for broad-scope asymmetric reactions that are needed for synthetic manipulations of complex molecules.

ASSOCIATED CONTENT

Supporting Information

. The Supporting Information is available free of charge on the ACS Publications website at DOI: 10.1021/jacs.5b09225.

Experimental procedures including synthesis and characterization of ligand **L2**, BINAP-dMOF (**II**), and nitro-MOF (**III**), procedures for BINAP-MOF·Rh (**I**·Rh)-catalyzed reductive cyclization and Alder-ene cycloisomerization, BINAP-dMOF·Rh (**II**·Rh)-catalyzed Pauson–Khand-type reaction, and recycling experiment of Pauson–Khand-type reaction with **II**·Rh, and HPLC traces of all products (PDF)

Crystallographic data (CIF)

AUTHOR INFORMATION

Corresponding Author

*wenbinlin@uchicago.edu

Notes

The authors declare no competing financial interest.

ACKNOWLEDGMENTS

This work was supported by NSF (CHE-1464941). We thank C. Poon and C. W. Abney for help with ICP-MS analyses. We acknowledge Dr. I. Bolotin (University of Illinois at Chicago) for help with optical rotation measurements. Single crystal diffraction studies were performed at ChemMatCARS (Sector 15), APS, Argonne National Laboratory. ChemMatCARS is principally supported by the Divisions of Chemistry (CHE) and Materials Research (DMR), National Science Foundation, under grant no. NSF/CHE-1346572. XAFS studies were performed at beamlines 20BM-B at the APS (Sector 20). Sector 20 operations are supported by the U.S. Department of Energy and the Canadian Light Source, with additional support from the University of Washington. Use of the APS, an Office of Science User Facility operated for the U.S. DOE Office of Science by Argonne National Laboratory, was supported by the U.S. DOE under contract no. DE-AC02-06CH11357.

REFERENCES

(1) (a) Suh, M. P.; Park, H. J.; Prasad, T. K.; Lim, D.-W. *Chem. Rev.* **2012**, *112*, 782. (b) Sumida, K.; Rogow, D. L.; Mason, J. A.; McDonald, T. M.; Bloch, E. D.; Herm, Z. R.; Bae, T.-H.; Long, J. R. *Chem. Rev.* **2012**, *112*, 724. (c) Dincă, M.; Long, J. R. *Angew. Chem., Int. Ed.* **2008**, *47*, 6766. (d) Rowsell, J. L. C.; Yaghi, O. M. *Angew. Chem., Int. Ed.* **2005**, *44*, 4670.

(2) (a) Liu, D.; Lu, K.; Poon, C.; Lin, W. *Inorg. Chem.* **2014**, *53*, 1916. (b) Kreno, L. E.; Leong, K.; Farha, O. K.; Allendorf, M.; Van Duyne, R. P.; Hupp, J. T. *Chem. Rev.* **2012**, *112*, 1105. (c) Cui, Y.; Yue, Y.; Qian, G.; Chen, B. *Chem. Rev.* **2012**, *112*, 1126. (d) Allendorf, M. D.; Bauer, C. A.; Bhakta, R. K.; Houk, R. J. T. *Chem. Soc. Rev.* **2009**, *38*, 1330.

(3) Rocca, J. D.; Lin, W. *Eur. J. Inorg. Chem.* **2010**, *2010*, 3725.

(4) (a) Horcajada, P.; Gref, R.; Baati, T.; Allan, P. K.; Maurin, G.; Couvreur, P.; Férey, G.; Morris, R. E.; Serre, C. *Chem. Rev.* **2012**, *112*, 1232. (b) Rocca, J. D.; Liu, D.; Lin, W. *Acc. Chem. Res.* **2011**, *44*, 957. (c) Huxford, R. C.; Rocca, J. D.; Lin, W. *Curr. Opin. Chem. Biol.* **2010**, *14*, 262.

(5) (a) Wang, C.; Zhang, T.; Lin, W. *Chem. Rev.* **2012**, *112*, 1084. (b) Evans, O. R.; Lin, W. *Acc. Chem. Res.* **2002**, *35*, 511.

(6) (a) Gascon, J.; Corma, A.; Kapteijn, F.; Llabrés i Xamena, F. X. *ACS Catal.* **2014**, *4*, 361. (b) Zhao, M.; Ou, S.; Wu, C.-D. *Acc. Chem. Res.* **2014**, *47*, 1199. (c) Yoon, M.; Srirambalaji, R.; Kim, K. *Chem. Rev.* **2012**, *112*, 1196. (d) Falkowski, J. M.; Liu, S.; Lin, W. *Isr. J. Chem.* **2012**, *52*, 591. (e) Ma, L.; Abney, C.; Lin, W. *Chem. Soc. Rev.* **2009**, *38*, 1248. (f) Lee, J.; Farha, O. K.; Roberts, J.; Scheidt, K. A.; Nguyen, S. T.; Hupp, J. T. *Chem. Soc. Rev.* **2009**, *38*, 1450.

(7) (a) Beyzavi, M. H.; Klet, R. C.; Tussupbayev, S.; Borycz, J.; Vermeulen, N. A.; Cramer, C. J.; Stoddart, J. F.; Hupp, J. T.; Farha, O. K. *J. Am. Chem. Soc.* **2014**, *136*, 15861. (b) Manna, K.; Zhang, T.; Carboni, M.; Abney, C. W.; Lin, W. *J. Am. Chem. Soc.* **2014**, *136*, 13182. (c) Manna, K.; Zhang, T.; Lin, W. *J. Am. Chem. Soc.* **2014**, *136*, 6566. (d) Fei, H.; Shin, J.; Meng, Y. S.; Adelhardt, M.; Sutter, J.; Meyer, K.; Cohen, S. M. *J. Am. Chem. Soc.* **2014**, *136*, 4965. (e) Falkowski, J. M.; Sawano, T.; Zhang, T.; Tsun, G.; Chen, Y.; Lockard, J. V.; Lin, W. *J. Am. Chem. Soc.* **2014**, *136*, 5213. (f) Mo, K.; Yang, Y.; Cui, Y. *J. Am. Chem. Soc.* **2014**, *136*, 1746. (g) Genna, D. T.; Wong-Foy, A. G.; Matzger, A. J.; Sanford, M. S. *J. Am. Chem. Soc.* **2013**, *135*, 10586. (h) Zhu, C.; Yuan, G.; Chen, X.; Yang, Z.; Cui, Y. *J. Am. Chem. Soc.* **2012**, *134*, 8058. (i) Kong, G.-Q.; Ou, S.; Zou, C.; Wu, C.-D. *J. Am. Chem. Soc.* **2012**, *134*, 19851. (j) Zheng, M.; Liu, Y.; Wang, C.; Liu, S.; Lin, W. *Chem. Sci.* **2012**, *3*, 2623. (k) Wang, C.; Wang, J.-L.; Lin, W. *J. Am. Chem. Soc.* **2012**, *134*, 19895. (l) Fateeva, A.; Chater, P. A.; Ireland, C. P.; Tahir, A. A.; Khimyak, Y. Z.; Wiper, P.

DOI: 10.1021/jacs.5b09225
J. Am. Chem. Soc. 2015, 137, 12241–12248

V.; Darwent, J. R.; Rosseinsky, M. J. *Angew. Chem., Int. Ed.* **2012**, *51*, 7440.
(8) (a) Cavka, J. H.; Jakobsen, S.; Olsbye, U.; Guillou, N.; Lamberti, C.; Bordiga, S.; Lillerud, K. P. *J. Am. Chem. Soc.* **2008**, *130*, 13850. (b) Kandiah, M.; Nilsen, M. H.; Usseglio, S.; Jakobsen, S.; Olsbye, U.; Tilset, M.; Larabi, C.; Quadrelli, E. A.; Bonino, F.; Lillerud, K. P. *Chem. Mater.* **2010**, *22*, 6632.
(9) For other chelating phosphine-based MOFs, see: Bohnsack, A. M.; Ibarra, I. A.; Bakhmutov, V. I.; Lynch, V. M.; Humphrey, S. M. *J. Am. Chem. Soc.* **2013**, *135*, 16038.
(10) (a) Seo, J. S.; Whang, D.; Lee, H.; Jun, S. I.; Oh, J.; Jeon, Y. J.; Kim, K. *Nature* **2000**, *404*, 982. (b) Hu, A.; Ngo, H. L.; Lin, W. *J. Am. Chem. Soc.* **2003**, *125*, 11490. (c) Wu, C.-D.; Hu, A.; Zhang, L.; Lin, W. *J. Am. Chem. Soc.* **2005**, *127*, 8940. (d) Cho, S.-H.; Ma, B.; Nguyen, S. T.; Hupp, J. T.; Albrecht-Schmitt, T. E. *Chem. Commun.* **2006**, 2563. (e) Wu, C.-D.; Lin, W. *Angew. Chem., Int. Ed.* **2007**, *46*, 1075. (f) Ma, L.; Falkowski, J. M.; Abney, C.; Lin, W. *Nat. Chem.* **2010**, *2*, 838. (g) Song, F.; Wang, C.; Falkowski, J. M.; Ma, L.; Lin, W. *J. Am. Chem. Soc.* **2010**, *132*, 15390. (h) Dang, D.; Wu, P.; He, C.; Xie, Z.; Duan, C. *J. Am. Chem. Soc.* **2010**, *132*, 14321. (i) Song, F.; Wang, C.; Lin, W. *Chem. Commun.* **2011**, *47*, 8256. (j) Falkoeski, J. M.; Wang, C.; Liu, S.; Lin, W. *Angew. Chem., Int. Ed.* **2011**, *50*, 8674.
(11) (a) Watson, I. D. G.; Toste, F. D. *Chem. Sci.* **2012**, *3*, 2899. (b) Marinetti, A.; Jullien, H.; Voituriez, A. *Chem. Soc. Rev.* **2012**, *41*, 4884. (c) Belmont, P.; Parker, E. *Eur. J. Org. Chem.* **2009**, *2009*, 6075. (d) Shen, H. C. *Tetrahedron* **2008**, *64*, 7847. (e) Jiménez-Núñez, E.; Echavarren, A. M. *Chem. Rev.* **2008**, *108*, 3326. (f) Michelet, V.; Toullec, P. Y.; Genêt, J.-P. *Angew. Chem., Int. Ed.* **2008**, *47*, 4268. (g) Aubert, C.; Buisine, O.; Malacria, M. *Chem. Rev.* **2002**, *102*, 813. (h) Trost, B. M.; Krische, M. J. *Synlett* **1998**, *1998*, 1. (i) Ojima, I.; Tzamarioudaki, M.; Li, Z.; Donovan, R. J. *Chem. Rev.* **1996**, *96*, 635. (j) Trost, B. M. *Acc. Chem. Res.* **1990**, *23*, 34.
(12) (a) Trost, B. M. *Angew. Chem., Int. Ed. Engl.* **1995**, *34*, 259. (b) Trost, B. M. *Acc. Chem. Res.* **2002**, *35*, 695.
(13) (a) Nakanishi, K.; Goto, T.; Ito, S.; Nozoe, S. In *Natural Product Chemistry*; Kodansha: Tokyo, 1974; Vols. *I*–*III*. (b) *Dictionary of Natural Products*, 1st ed.; Buckingham, J., Ed.; Chapman & Hall: New York, 1994.
(14) (a) Jang, H.-Y.; Krische, M. J. *J. Am. Chem. Soc.* **2004**, *126*, 7875. (b) Jang, H.-Y.; Hughes, F. W.; Gong, H.; Zhang, J.; Brodbelt, J. S.; Krische, M. J. *J. Am. Chem. Soc.* **2005**, *127*, 6174.
(15) (a) Cao, P.; Zhang, X. *Angew. Chem., Int. Ed.* **2000**, *39*, 4104. (b) Lei, A.; He, M.; Wu, S.; Zhang, X. *Angew. Chem., Int. Ed.* **2002**, *41*, 3457. (c) Lei, A.; He, M.; Zhang, X. *J. Am. Chem. Soc.* **2002**, *124*, 8198. (d) Lei, A.; Waldkirch, J. P.; He, M.; Zhang, X. *Angew. Chem., Int. Ed.* **2002**, *41*, 4526. (e) Lei, A.; He, M.; Zhang, X. *J. Am. Chem. Soc.* **2003**, *125*, 11472. (f) He, M.; Lei, A.; Zhang, X. *Tetrahedron Lett.* **2005**, *46*, 1823.
(16) For Rh-catalyzed asymmetric Pauson–Khand reaction, see: (a) Jeong, N.; Sung, B. K.; Choi, Y. K. *J. Am. Chem. Soc.* **2000**, *122*, 6771. For examples of Rh-catalyzed Pauson–Khand reactions by use of aldehydes instead of carbon monoxide, see: (b) Morimoto, T.; Fuji, K.; Tsutsumi, K.; Kakiuchi, K. *J. Am. Chem. Soc.* **2002**, *124*, 3806. (c) Shibata, T.; Toshida, N.; Takagi, K. *Org. Lett.* **2002**, *4*, 1619. (d) Shibata, T.; Toshida, N.; Takagi, K. *J. Org. Chem.* **2002**, *67*, 7446.
(17) For reviews of Pauson–Khand reactions, see: (a) Lee, H.-W.; Kwong, F.-Y. *Eur. J. Org. Chem.* **2010**, *2010*, 789. (b) Park, J. H.; Chang, K.-M.; Chung, Y. K. *Coord. Chem. Rev.* **2009**, *253*, 2461. (c) Strübing, D.; Beller, M. *Top. Organomet. Chem.* **2006**, *18*, 165. (d) Gibson, S. E.; Mainolfi, N. *Angew. Chem., Int. Ed.* **2005**, *44*, 3022. (e) Blanco-Urgoiti, J.; Añorbe, L.; Pérez-Serrano, L.; Dominguez, G.; Pérez-Castells, J. *Chem. Soc. Rev.* **2004**, *33*, 32. (f) Brummond, K. M.; Kent, J. L. *Tetrahedron* **2000**, *56*, 3263. (g) Chung, Y. K. *Coord. Chem. Rev.* **1999**, *188*, 297. (h) Geis, O.; Schmalz, H.-G. *Angew. Chem., Int. Ed.* **1998**, *37*, 911.
(18) (a) Zhang, X.; Llabrés i Xamena, F. X.; Corma, A. *J. Catal.* **2009**, *265*, 155. (b) Vermoortele, F.; Vandichel, M.; de Voorde, B. V.; Ameloot, R.; Waroquier, M.; Van Speybroeck, V.; De Vos, D. E. *Angew. Chem., Int. Ed.* **2012**, *51*, 4887. (c) Václacík, J.; Servalli, M.; Lothschütz, C.; Szlachetko, J.; Ranocchiari, M.; van Bokhoven, J. A. *ChemCatChem* **2013**, *5*, 692. (d) Vermoortele, F.; Bueken, B.; Le Bars, G.; Van de Voorde, B.; Vandichel, M.; Houthoofd, K.; Vimont, A.; Daturi, M.; Waroquier, M.; Van Speybroeck, V.; Kirschhock, C.; De Vos, D. E. *J. Am. Chem. Soc.* **2013**, *135*, 11465.
(19) **II**·Rh(BF_4) gave 84% yield of **2f**, whereas a similar result was obtained for the reaction with a smaller substrate **1a** (69% of the desired product and byproducts).
(20) **II**·Rh(SbF_6) afforded 81% yield of **4f**, whereas meaning improvement was not observed for the reaction of a smaller substrate **3a** at 0.1 mol% Rh loading (44% yield with **II**·Rh(SbF_6) versus 38% yield with **I**·Rh(SbF_6)).
(21) **II**·RhCl-catalyzed Pauson–Khand reaction under CO also did not proceed.
(22) (a) Deng, H.; Doonan, C. J.; Furukawa, H.; Ferreira, R. B.; Towne, J.; Knobler, C. B.; Wang, B.; Yaghi, O. M. *Science* **2010**, *327*, 846. (b) Wang, C.; Liu, D.; Xie, Z.; Lin, W. *Inorg. Chem.* **2014**, *53*, 1331. (c) Manna, K.; Zhang, T.; Greene, F. X.; Lin, W. *J. Am. Chem. Soc.* **2015**, *137*, 2665.
(23) Dierschke, F.; Grimsdale, A. C.; Müllen, K. *Synthesis* **2003**, 2470.
(24) Férey, G.; Mellot-Draznieks, C.; Serre, C.; Millange, F. *Acc. Chem. Res.* **2005**, *38*, 217.
(25) Yoon, T. P.; Jacobsen, E. N. *Science* **2003**, *299*, 1691.

DOI: 10.1021/jacs.5b09225
J. Am. Chem. Soc. 2015, 137, 12241–12248